ACS Macro Letters

Editors' Choice

pubs.acs.org/macroletters

Letter

Impact of a Lightly Branched Star Polyelectrolyte Architecture on Polyelectrolyte Complexes

Kaden C. Stevens* and Matthew V. Tirrell*

Cite This: *ACS Macro Lett.* 2024, 13, 688−694

Read Online

ACCESS | Metrics & More | Article Recommendations | Supporting Information

ABSTRACT: The effect of charge density in blocky and statistical linear polyelectrolytes on polyelectrolyte complex (PEC) properties has been studied with the finding that increased charge density in a polyelectrolyte tends to increase the salt resistance and modulus of a PEC across various polyelectrolyte pairs. Here, we demonstrate the ability to orthogonally alter PEC salt resistance while maintaining rheological properties and internal structure by going from linear to lightly branched architectures with similar total degrees of polymerization. Using a model system built around glycidyl methacrylate (GMA) and thiol-epoxy "click" functionalization, we create a library of homologous linear, 4-armed, 6-armed, and 8-armed star polyelectrolytes. The PECs formed from these model polyelectrolyte pairs are then characterized via optical microscopy, rheology, and small-angle X-ray scattering to evaluate their salt resistance, mechanical properties, and internal structure. We argue that our results are due to the difference between linear charge density or charge per unit length along backbone segments for each polyelectrolyte and spatial charge density, the number of charges per unit volume of the polyelectrolyte prior to complexation. Our findings suggest that linear charge density is the dominant factor in determining intermolecular interactions of the complex, leading to identical rheological and structural behavior, whereas the spatial charge density primarily influences the stability of the complexes. These distinct mechanisms for altering various sought-after PEC properties offer greater potential applications in precision design of polyelectrolyte complex materials.

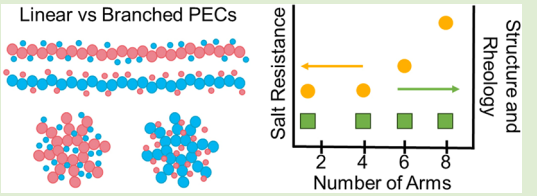

Polyelectrolyte complexes (PECs) are dense, water-swollen, polymer-rich phases spontaneously formed upon mixing oppositely charged polyelectrolytes.[1−3] Since polyelectrolyte complexation is an associative phase separation process based primarily on charge−charge interactions, PECs can incorporate a variety of organic, inorganic, and biologic-charged molecules, making them attractive candidates for applications in nucleic acid delivery, underwater adhesives, and nanoscale reactors.[4−9] However, the rational design of PECs remains difficult, as their properties depend on a complex interplay between environmental factors such as solvent mixture, salinity, pH, and temperature in addition to the variety of supramolecular interactions between the oppositely charged polyelectrolytes.[10,11] Recently, there has been a surge in interest toward using structural features of polyelectrolytes, such as length, charge density, and charge blockiness, to alter the stability, rheology, and structure of PEC materials.[12−16] Structure−property relationships centered on polyelectrolyte design are attractive because they can provide robust, chemically agnostic design principles for PECs and provide a path toward tailored PEC design within applications where environmental conditions are beyond control.[17] Polyelectrolyte charge density is one of the most promising parameters recently investigated, as it has been shown to consistently alter the rheology and stability of PECs.[17,18]

By copolymerizing charged monomers with neutral monomers, one can reduce the charge density of the constituent polyelectrolytes within PEC domains. Reducing charge density this way alters linear charge density or charge density along the polymer backbone and results in PECs with a lower modulus and a reduced salt resistance compared to their fully charged counterparts.[17] PEC modulus is highly sensitive to the number of ionic pairings between polymers, which act as stickers between oppositely charged polymer chains, increasing the viscosity of the PEC.[12,13,19,20] Lowering charge density reduces sticker density, providing a straightforward path to weaken mechanical properties. PEC stability is also related to charge density, but that mechanism is generally rationalized through the influence of charge density on counterion dynamics, not electrostatic interactions.[21,22]

Before complexation, the charged groups along a polyelectrolyte backbone experience significant electrostatic repulsion.[2] In solution, small molecule counterions and water molecules condense around charged groups along the polyelectrolyte backbone to reduce the effective charge density along the chain. Upon complexation, oppositely charged polyelectrolytes con-

Received: March 18, 2024
Revised: May 9, 2024
Accepted: May 14, 2024
Published: May 23, 2024

dense around each other to mediate electrostatic repulsion, releasing the small molecules and restoring their translational entropy. The entropic gain from counterion release is the majority of the thermodynamic driving force for polyelectrolyte complexation and is directly related to the amount of salt a PEC can withstand before dissolution, otherwise known as the critical salt concentration (CSC).[22] The significant role of counterion release in the complexation process allows one to tune the stability of a PEC by altering the charge density of the constituent polyelectrolytes.

Reducing charge density through copolymerization with a neutral monomer weakens charge−charge interactions along a polyelectrolyte, reducing counterion condensation in solution and thus the translational entropy gain from complexation, leading to PECs with lower CSCs.[2,3,22] Interestingly, the CSC is not only sensitive to linear charge density, but also spatial charge density or the distribution of charged groups in space.[23] Chang et al. showed that increased blockiness raises PEC salt resistance by creating PECs from sequence-defined copolymers with identical charged fractions, but increasingly blocky charged sequences.[22] They attributed this result to stronger interactions between counterions and charged groups in the blocky sequences, reasoning charged groups clustered closely together would experience more electrostatic repulsion relative to charged groups spaced evenly apart. While this illustrates an important point, altering charge sequences can only vary the stability of copolyelectrolytes. There are essentially no tuning parameters to alter the CSC of PECs composed of linear, fully charged polyelectrolytes. The CSC of fully charged polyelectrolytes show a pronounced dependence on degree of polymerization (DP) at low molecular weights, which quickly plateaus to nearly constant values at higher DPs.[3] Since the salt resistance of a PEC determines the limits of the environments where it can be used, a reliable method to increase complex stability beyond the DP limited plateau value would be advantageous to molecular engineering design strategies.

No studies have addressed methods to increase the charge density beyond what can be attained in linear, fully charged polyelectrolytes for use in bulk PECs. It is conceivable one could design multivalent monomers, but this approach would be synthetically challenging to apply to a variety of charged groups. Instead, we were inspired to investigate macromolecular architecture from molecular dynamics simulations that showed branched polyelectrolytes, compared to linear counterparts, exhibit greater spatial charge density and perturb counterions more strongly relative to linear polyelectrolytes.[24] However, no experimental reports have validated these consequences on bulk PEC properties. Here, we seek to increase the spatial charge density of homopolyelectrolytes by altering their architecture from linear to lightly branched stars, in the hope of precisely tuning PEC properties. We find spatial charge density to have a significant impact on the salt stability of our complexes while leaving the viscoelastic and structural properties of our complexes essentially unaltered, which suggests that linear and spatial charge density may play distinct roles in determining PEC properties.

To investigate the effect of a polyelectrolyte architecture on PECs, we chose to create homologous polyelectrolyte pairs via a combination of reactive polymers and click chemistry. This approach allows us to limit structural variation between polyelectrolyte pairs within our PECs and has been used extensively in recent years.[17,18,25−28] However, many reactive polymer platforms suffer from inefficient functionalization, poor polymerization control, or unstable reactive groups.[16,17] For this reason, we chose to create a new homologous polyelectrolyte platform based on poly(glycidyl methacrylate) (PGMA).

PGMA stands out as an ideal reactive platform because it is readily synthesized via controlled radical polymerization (CRP) techniques and is stable upon storage in air and moisture for extended periods of time.[29,30] In addition, the pendant epoxy groups undergo rapid and quantitative thiol-epoxy functionalization in the presence of a small excess of thiol and catalytic base (Scheme 1).[29,31] Finally, every thiol-epoxy reaction creates a

Scheme 1. Route Towards Homologous Polyelectrolytes through PolyGMA and Thiol-Epoxy

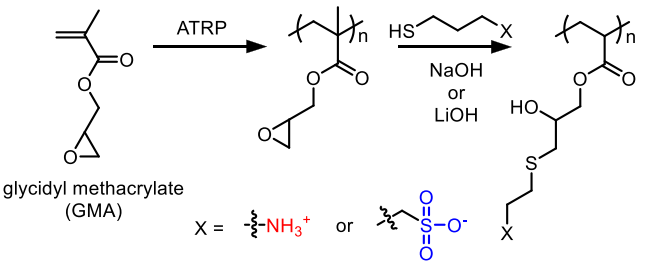

thioether bond that can be oxidized to alter local polarity and a secondary hydroxyl group, which can serve as a reactive handle for additional functionalization reactions.[29,32,33]

We synthesized PGMA via atom-transfer radical polymerization (ATRP) according to previously reported procedures.[32] To achieve cationic derivatives of PGMA, we react 2-(Boc-amino)ethanethiol in THF using LiOH as a base with a ratio of epoxy/thiol/base of 1:4:0.05. The Boc-protected PGMA derivative was deprotected using a 1:1 mixture of dioxane/6 M HCl, leading to a cationic derivative of PGMA bearing primary amines as cationic groups (Figure S1). Typically, cationic derivatives of PGMA are achieved by deprotection using trifluoroacetic acid (TFA).[34,35] We chose to use HCl instead to avoid residual TFA counterions that are challenging to remove. To create anionic PGMA derivatives, we reacted PGMA with sodium 3-mercapto-1-propanesulfonate at an epoxy/thiol ratio of 1:4 in a DMSO/H_2O mixture. Slow addition of 0.1 equiv of aqueous NaOH to epoxy drove quantitative sulfonate functionalization of PGMA (Figure S1). To the best of our knowledge, this is the first report of anionic derivatization of PGMA through a thiol-epoxy mechanism. Next, we synthesized a series of well-defined linear, 4-armed, 6-armed, and 8-armed PGMA with low dispersity ($Đ < 1.14$) via ATRP (Figure 1 and Table S1). We targeted 200 GMA units across all architectures so that small changes in DP would not result in significant deviations of the CSC, since CSC generally follows the approximation $DP \sim \frac{1}{1-CSC}$.[36,37] This size range also ensures the arm length of the higher branched stars would remain quite short to test simulation results that show more highly branched polyelectrolytes with shorter arms affect counterion dynamics most strongly relative to linear polyelectrolytes with the same DP.[24] These reactive precursors were functionalized via thiol-epoxy into homologous polyelectrolyte pairs used throughout this study. For brevity, coacervate samples are labeled according to the reactive polymer precursor their constituent polyelectrolyte pairs were derived from (i.e., L-GMA for linear PGMA, 4-GMA for 4-armed PGMA, etc.).

Optical microscopy images allow us to assess the phase morphology of polyelectrolyte architectures as a function of salt.

https://doi.org/10.1021/acsmacrolett.4c00167
ACS Macro Lett. 2024, 13, 688−694

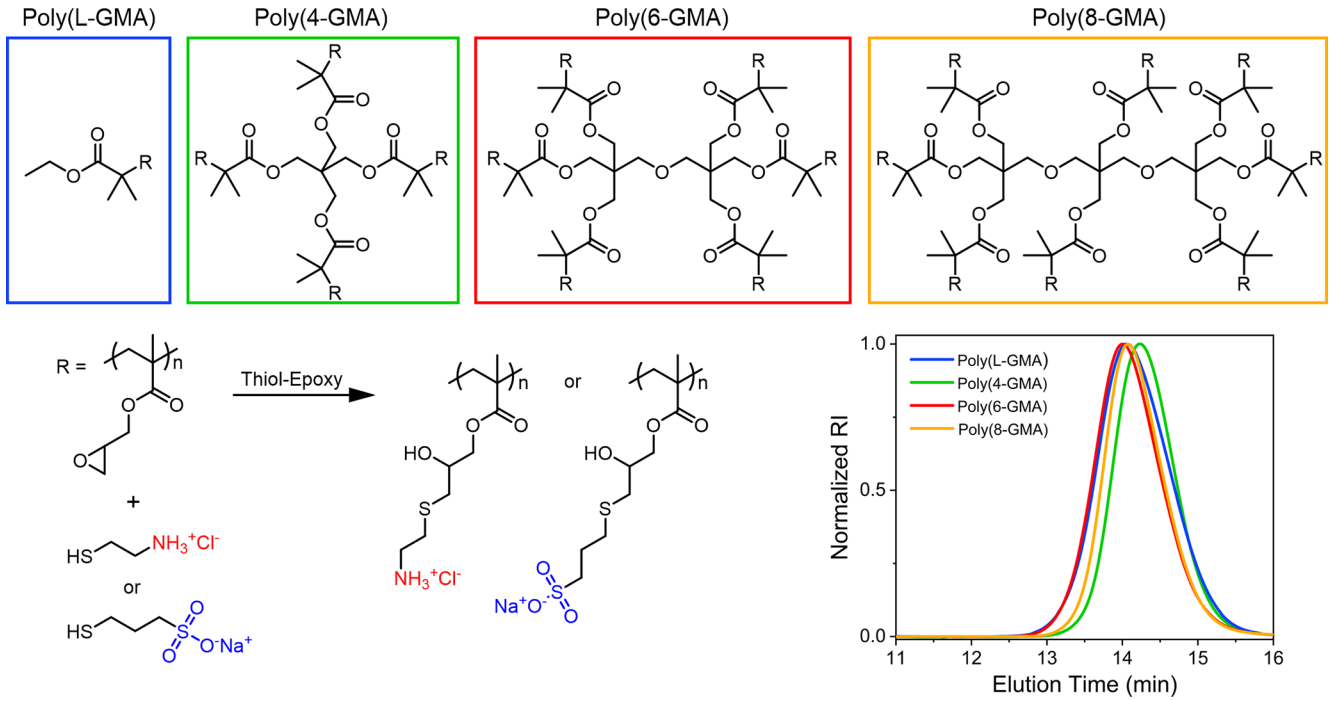

Figure 1. Synthetic scheme for linear and branched polyelectrolytes derived from PGMA. Overlaid size-exclusion chromatography traces of neutral PGMA with total degree of polymerization of ∼200 (Table S1; bottom right).

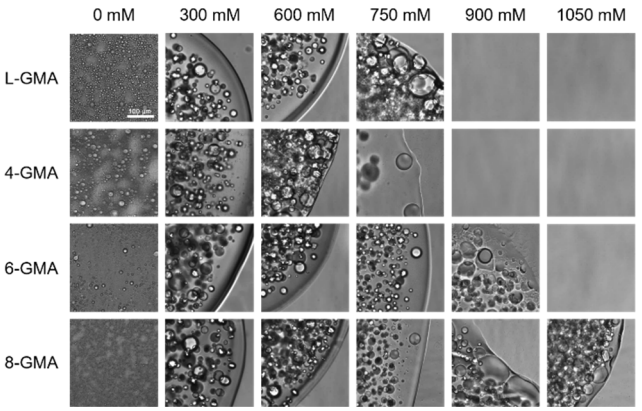

Figure 2. Optical micrographs of PECs composed of analogous polyelectrolytes derived from linear, 4-armed, 6-armed, and 8-armed GMA precursors at 0 to 1050 mM added salt concentrations. Scale bar in the bottom left corner of the top right image denotes 100 μm and this scale is consistent across all images.

In all cases, PECs are liquid-like coacervates at 10 mg/mL total polymer concentration (Figure 2). At no added salt, the complexes form spherical droplets. Upon the addition of external NaCl salt, the PEC phase coalesces with visual evidence of water droplets, a morphology observed in viscous liquid PECs.[11,17,38] Previous studies have shown that doubling the charge density of a constituent polyelectrolyte can drive a morphological transition from liquid to solid PECs.[39] Here, the PEC morphology is consistent across PEC architectures, indicating the lightly branch polyelectrolytes explored here do not increase charge density enough to alter PEC morphology.

To evaluate CSC values, we examined PECs of all architectures at increasing salt concentrations. Optical microscopy shows 6-GMA and 8-GMA have higher CSCs than L-GMA and 4-GMA. L-GMA and 4-GMA pairings persist until approximately 750 mM NaCl, whereas 6-GMA and 8-GMA persist until 900 and 1050 mM NaCl, respectively. The ∼50% increase in CSC from L-GMA to 8-GMA cannot be explained by the differences in molecular weight between the samples, as critical salt resistance scales modestly at higher molecular weights. This suggests architectural differences are the primary driving force for increased salt stability in these complexes, in line with previous observations of more compact charge distributions within a polyelectrolyte increasing the salt resistance of the resulting PEC.[22]

There are a few potential reasons why the CSC does not increase until 6-armed stars. First, the longer side chains of 4-GMA relative to 6-GMA and 8-GMA decrease the average charge density experienced by arms of 4-GMA, since the available space for each arm to occupy grows rapidly as chains extend radially from the polymer core. Similarly, the difference in CSC between 6- and 8-armed stars can be rationalized both by the increased number of arms radiating from the core and the shorter radial extension of 8-GMA increasing the steric congestion of charged groups relative to 6-GMA. Consequently, it is possible 4-armed stars may begin to exhibit distinct salt resistances from equivalent linear counterparts at lower DPs and more compact radial chain distributions. Regardless, we have identified a region where increased spatial charge density of polyelectrolytes can enhance the salt resistance of a bulk PEC material and now move on to investigate architecture effects on mechanical properties.

Viscoelastic properties of each complex were analyzed using small amplitude oscillatory shear (SAOS) experiments across time−temperatures superposition (TTS) from 5 to 75 °C (Figure 3). The complexes displayed rheological behavior typical of "sticky rouse" viscoelastic liquids, with storage modulus (G') and loss modulus (G'') scaling as $\omega^{0.5}$ at moderate to high frequencies ($\omega a_T > 10°$ rad/s) and G' and G'' scaling, respectively, as ω^2 and ω at low frequencies ($\omega a_T < 10°$

https://doi.org/10.1021/acsmacrolett.4c00167
ACS Macro Lett. 2024, 13, 688−694

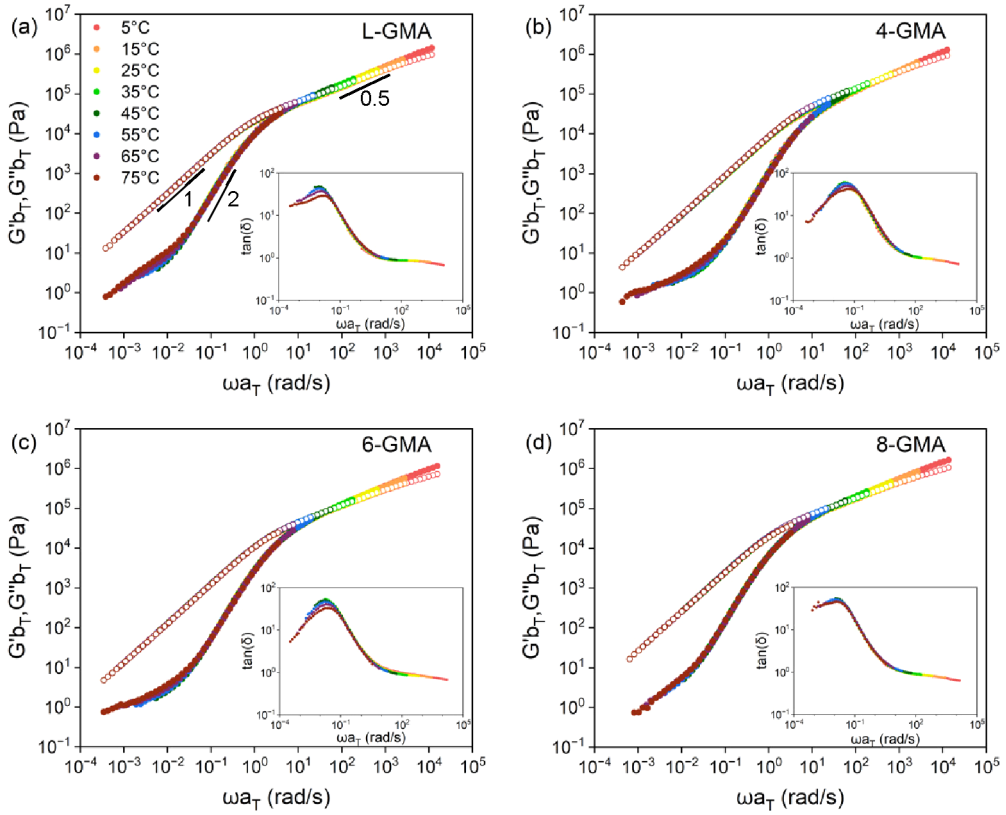

Figure 3. Time−temperature superposition (TTS) of frequency sweep data for 0 mM added NaCl PECs of (a) linear, (b) 4-armed, (c) 6-armed, and (d) 8-armed architectures (●,○ G',G''). Shift factors a_T and b_T are tabulated in Tables S3−S6.

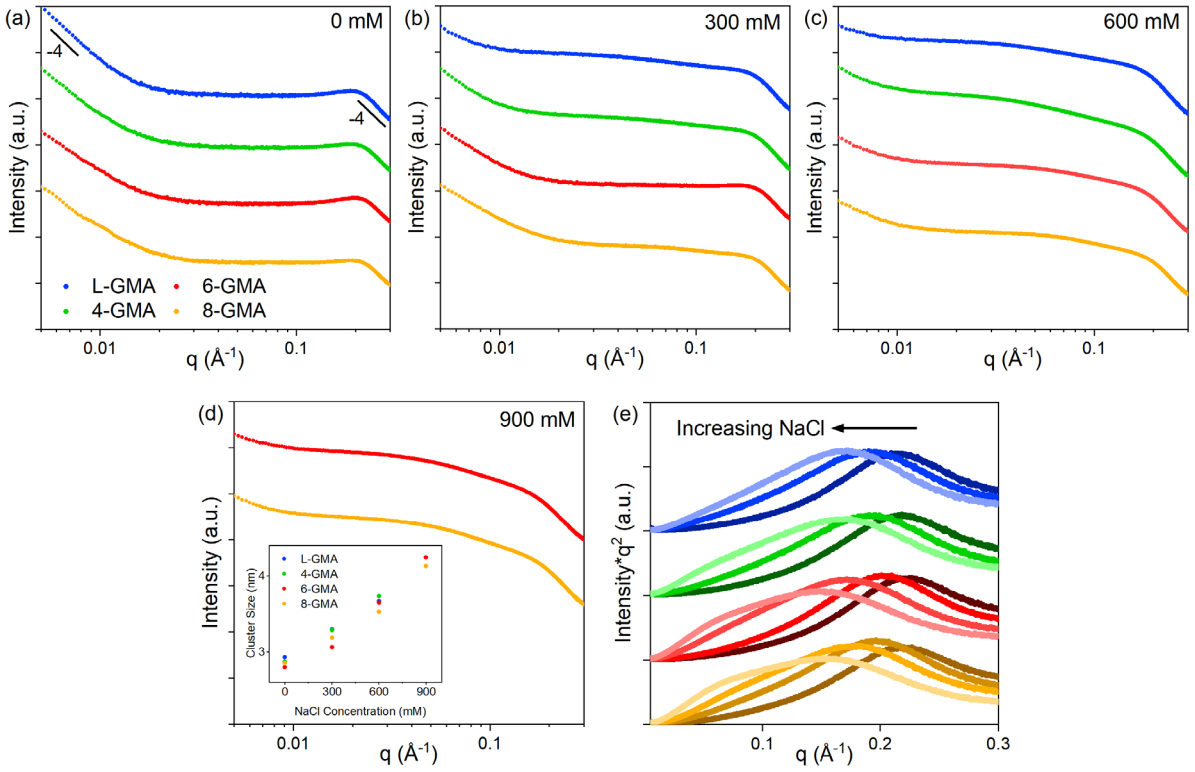

Figure 4. SAXS scattering patterns for polyelectrolyte pairs of every architecture at (a) 0, (b) 300, (c) 600, and (d) 900 mM added NaCl (inset figure shows the cluster size (R_g) corresponding to the onset of −4 slopes at high q). (e) Kratky plots of linear (blue), 4-armed (green), 6-armed (red), and 8-armed (gold) PECs (arranged from top to bottom). Lighter shades correspond to higher salt concentrations, which go from 0 to 900 mM NaCl in 300 mM steps.

https://doi.org/10.1021/acsmacrolett.4c00167
ACS Macro Lett. 2024, 13, 688−694

rad/s).[20] Interestingly, we observed notable deviations from traditional Rouse-like behavior in the TTS data.

First, we observe a crossover of G' and G'' at intermediate frequencies, which persists to the highest frequencies measured, reminiscent of entangled polymeric behavior. However, these materials are likely unentangled due to the relatively low molecular weight (26−31 kg/mol) of constituent polymers, alongside the presence of long side chains and the high water content swelling the network (Table S3). We believe this crossover is not due to entanglement, but instead due to "sticky" interactions between segments of polymer chains enhancing the solid character of our PECs. The chemical attributes of these polyelectrolyte side chains provide a variety of associative amphiphilic, hydrogen bonding and ionic intermolecular interactions which could contribute to this feature. Similar crossover signatures have been observed in other unentangled PEC systems capable of significant nonionic supramolecular interactions.[38,40]

Unentangled polymers G' and G'' are expected to scale as ω^2 and ω, respectively, in the terminal regime.[41] However, there is an upturn in G' at low frequencies which deviates from the expected scaling of ω^2. This additional relaxation mode has been reported before in PEC literature and is often attributed to long-range interactions or an instrument artifact.[17,37] Since the feature is not excessively noisy and is observed at torque values well above the sensitivity limit of our rheometer, we believe this upturn in storage modulus represents a secondary relaxation mode in our PECs. In other classes of materials such as associative protein hydrogels, low frequency upturns in storage modulus have been attributed to large sections of polymer chains with high valency interacting through long distances.[42] It is conceivable to envision fully charged homopolyelectrolytes sustaining intermolecular interactions between segments of multiple oppositely charged polyelectrolytes within a PEC, so this low frequency upturn in storage modulus is not surprising. Future work tuning this additional long-range relaxation mode by altering supramolecular interactions such as hydrogen bonding, $\pi-\pi$ stacking and amphiphilic associations in PECs will be necessary to fully explain this feature.

Lightly branched polyelectrolyte architectures do not systematically alter the shape of the SAOS data, shift factors or intrinsic viscosities of branched complexes relative to linear complexes (Figures 3 and S2−S4 and Tables S3−S6). This was initially surprising, since architectural variations from linear to branched polymers in uncharged systems is often accompanied by large differences in viscoelasticity emerging from a shift in entanglement mechanism from reptation to arm-retraction.[41,43] We attribute the identical behavior to the high water content and consistent intermolecular interactions across our PECs. Since PECs are water-swollen, entanglement requires much higher degrees of polymerization relative to unswollen polymer.[41] As a result, our materials are likely unentangled at this DP, which eliminates the primary difference in the diffusion of star and linear polymers. In addition, since all homopolyelectrolytes have approximately equal DP, the number and density of intrinsic ionic pairings known to dominate PEC dynamics should be approximately equal across all architectures. As a result, we see very consistent rheological profiles across all polyelectrolyte architectures.

Small-angle X-ray scattering (SAXS) allows us to examine how altering molecular architecture influences the internal structures of our PECs. Figure 4a−d shows vertically shifted overlays of SAXS patterns obtained from complexes of each architecture arranged by salt concentration. The SAXS patterns obtained for each complex are nearly identical at every salt concentration, with prominent features closely matching each other. In all cases, $I(q)$ scales as q^{-4} at low q ($q < 0.01$ Å^{-1}), suggesting smooth surfaces due to mesoscale concentration fluctuations with $R_g > 200$ nm (since $R_{g\_max} = 2\pi/q_{min}$). The prominent −4 slope persists to slightly higher q ranges as branching increases, suggesting the minimum size affected by these concentration fluctuations may be weakly influenced by architecture.

At high q ($q > 0.1$ Å^{-1}), we observe a peak that could be mistaken for a correlation peak indicating some average intermolecular distance within the complex. However, at higher q, we observe a $I(q) \sim q^{-4}$ scaling that suggests this peak corresponds to small, smooth aggregates within the material, a feature more akin to micellar associations than intermolecular spacings. The prominent peaks in the Kratky plots indicate collapsed, globular structures (Figure 4E). The absence of a gel-like rheological response suggests that these clusters are not permanent enough to form physical cross-links. We hypothesize that they may be transient, dynamic associations between monomers. The two aggregation mechanisms apparent via SAXS at low and high q might relate to the unexpected increases in G' observed in the crossover of G' at moderate frequencies and the uptick in G' at low frequencies, respectively. These observations open future opportunities to clarify the relationship between rheological features and aggregation in architecturally diverse PECs.

As salt is added, the low q upturn shifts to lower q values, and the correlation peak at high q shifts to lower q values with reduced intensity. Cluster size, estimated using the onset of a −2 slope in the Kratky plots, grows consistently as salt is increased from ∼2.8 nm at 0 mM to 4.2 nm at 900 mM. The trends across salt concentrations are also consistent for each polyelectrolyte architecture, even at 900 mM, even though 6-GMA is near its CSC at this salt concentration and 8-GMA is much farther away from dissolution. This suggests that PECs have similar internal structures regardless of their proximity to the CSC, assuming they have equivalent degrees of polymerization and linear charge density.

Our collective results indicate that polyelectrolyte architecture can significantly alter the thermodynamic stability of PECs while keeping structures and mechanical properties essentially unchanged. The influence of architecture on thermodynamic stability is consistent with previous experimental and simulation findings: increased spatial charge density increases PEC salt resistance, and branched polyelectrolytes drive the charge density higher than linear counterparts. We conclude that the increased steric congestion allows branched polyelectrolytes to perturb counterion dynamics more than linear analogues prior to complexation, leading to a greater degree of translational entropy gain during the complexation process. Meanwhile, the negligible influence of architecture on structure and rheology is likely a consequence of the prepared moderately long and lightly branched structures. As molecular weight increases, we would expect entanglement behavior of star polyelectrolytes and linear polyelectrolytes. However, since PECs are swollen by plasticizing water, the entanglement DP for star polyelectrolytes may be difficult to achieve synthetically. A more detailed understanding of the interplay between linear and spatial charge density could lead to increasingly precise PEC design, whereby the judicious incorporation of branched and statistical

https://doi.org/10.1021/acsmacrolett.4c00167
ACS Macro Lett. 2024, 13, 688−694

copolyelectrolytes enables the rational design of PEC materials with orthogonal control over a range of CSCs and mechanical properties.

In this work, we evaluated the effect of polyelectrolyte architecture on PEC properties using homologous polyelectrolytes derived from the combination of thiol-epoxy and PGMA. The ease of PGMA synthesis and thiol-epoxy functionalization provides a straightforward pathway to homologous polyelectrolytes of various architectures. PECs from PGMA precursors produced viscous liquid complexes with architecture-dependent CSC. In contrast, the rheology and structure of our PECs measured by SAOS and SAXS was consistent across architectures. Together, our results suggest salt resistance can be selectively altered by incorporating lightly branched polyelectrolytes in PECs, presenting a pathway for precise modification of PEC properties. Furthermore, our results suggest a fundamental difference between the structure–property relationships resulting from variations in linear charge density through copolymerization and those arising from altered spatial charge density through polyelectrolyte architecture.

■ ASSOCIATED CONTENT

Supporting Information

The Supporting Information is available free of charge at https://pubs.acs.org/doi/10.1021/acsmacrolett.4c00167.

Experimental details and NMR, GPC, thermogravimetric, and rheology data (PDF)

■ AUTHOR INFORMATION

Corresponding Authors

Kaden C. Stevens − *Pritzker School of Molecular Engineering, The University of Chicago, Chicago, Illinois 60637, United States;* Present Address: Department of Chemistry, University of Florida, Gainesville, Florida 32611, United States; orcid.org/0000-0002-5853-8765; Email: kadenstevens@ufl.edu

Matthew V. Tirrell − *Pritzker School of Molecular Engineering, The University of Chicago, Chicago, Illinois 60637, United States;* orcid.org/0000-0001-6185-119X; Email: mtirrell@uchicago.edu

Complete contact information is available at: https://pubs.acs.org/10.1021/acsmacrolett.4c00167

Funding

This work was performed under the following financial assistance Award 70NANB19H005 from U.S. Department of Commerce, National Institute of Standards and Technology as part of the Center for Hierarchical Materials Design (CHiMaD). This work made use of the shared facilities at the University of Chicago Materials Research Science and Engineering Center, supported by National Science Foundation under Award Number DMR-2011854.

Notes

The authors declare no competing financial interest.

■ ACKNOWLEDGMENTS

Parts of this work were carried out at the Soft Matter Characterization Facility of the University of Chicago. The authors would like to thank Dr. Xiaobing Zuo for assistance collecting SAXS data at Argonne National Laboratory Advanced Photon Source beamline 12-ID-B. This work used resources of the Advanced Photon Source, a U.S. Department of Energy (DOE) Office of Science User Facility operated for the DOE Office of Science by Argonne National Laboratory under Contract No. DE-AC02-06CH11357.

■ REFERENCES

(1) Srivastava, S.; Tirrell, M. V. Polyelectrolyte Complexation. In *Advances in Chemical Physics*; Rice, S. A., Dinner, A. R., Eds.; John Wiley & Sons, Inc., 2016; Vol. *161*, pp 499−544.

(2) Muthukumar, M. 50th Anniversary Perspective: A Perspective on Polyelectrolyte Solutions. *Macromolecules* **2017**, *50* (24), 9528−9560.

(3) Sing, C. E.; Perry, S. L. Recent progress in the science of complex coacervation. *Soft Matter* **2020**, *16* (12), 2885−2914.

(4) Peters, D.; Kastantin, M.; Kotamraju, V. R.; Karmali, P. P.; Gujraty, K.; Tirrell, M.; Ruoslahti, E. Targeting atherosclerosis by using modular, multifunctional micelles. *Proc. Natl. Acad. Sci. U. S. A.* **2009**, *106* (24), 9815−9819.

(5) Zhou, Z.; Yeh, C.-F.; Mellas, M.; Oh, M.-J.; Zhu, J.; Li, J.; Huang, R.-T.; Harrison, D. L.; Shentu, T.-P.; Wu, D.; et al. Targeted polyelectrolyte complex micelles treat vascular complications in vivo. *Proc. Natl. Acad. Sci. U. S. A.* **2021**, *118* (50), No. e2114842118.

(6) Maggi, F.; Ciccarelli, S.; Diociaiuti, M.; Casciardi, S.; Masci, G. Chitosan nanogels by template chemical cross-linking in polyion complex micelle nanoreactors. *Biomacromolecules* **2011**, *12* (10), 3499−3507.

(7) Lindhoud, S.; Norde, W.; Cohen Stuart, M. A. Effects of polyelectrolyte complex micelles and their components on the enzymatic activity of lipase. *Langmuir* **2010**, *26* (12), 9802−9808.

(8) van Hees, I. A.; Hofman, A. H.; Dompé, M.; van der Gucht, J.; Kamperman, M. Temperature-responsive polyelectrolyte complexes for bio-inspired underwater adhesives. *Eur. Polym. J.* **2020**, *141*, No. 110034.

(9) Zhao, Q.; Lee, D. W.; Ahn, B. K.; Seo, S.; Kaufman, Y.; Israelachvili, J. N.; Waite, J. H. Underwater contact adhesion and microarchitecture in polyelectrolyte complexes actuated by solvent exchange. *Nature materials* **2016**, *15* (4), 407−412.

(10) Li, L.; Rumyantsev, A. M.; Srivastava, S.; Meng, S.; De Pablo, J. J.; Tirrell, M. V. Effect of Solvent Quality on the Phase Behavior of Polyelectrolyte Complexes. *Macromolecules* **2021**, *54* (1), 105−114.

(11) Meng, S.; Liu, Y.; Yeo, J.; Ting, J. M.; Tirrell, M. V. Effect of mixed solvents on polyelectrolyte complexes with salt. *Colloid Polym. Sci.* **2020**, *298* (7), 887−894.

(12) Akkaoui, K.; Yang, M.; Digby, Z. A.; Schlenoff, J. B. Ultraviscosity in Entangled Polyelectrolyte Complexes and Coacervates. *Macromolecules* **2020**, *53* (11), 4234−4246.

(13) Yang, M.; Shi, J.; Schlenoff, J. B. Control of Dynamics in Polyelectrolyte Complexes by Temperature and Salt. *Macromolecules* **2019**, *52* (5), 1930−1941.

(14) Stevens, K. C.; Tirrell, M. V. Structure and properties of bottlebrush polyelectrolyte complexes. *J. Polym. Sci.* **2023**, *1*, na.

(15) Stevens, K. C.; Marras, A. E.; Campagna, T. R.; Ting, J. M.; Tirrell, M. V. Effect of charged block length mismatch on double diblock polyelectrolyte complex micelle cores. *Macromolecules* **2023**, *56* (14), 5557−5566.

(16) Neitzel, A. E.; Fang, Y. N.; Yu, B.; Rumyantsev, A. M.; de Pablo, J. J.; Tirrell, M. V. Polyelectrolyte complex coacervation across a broad range of charge densities. *Macromolecules* **2021**, *54* (14), 6878−6890.

(17) Huang, J.; Morin, F. J.; Laaser, J. E. Charge-Density-Dominated Phase Behavior and Viscoelasticity of Polyelectrolyte Complex Coacervates. *Macromolecules* **2019**, *52* (13), 4957−4967.

(18) Huang, J.; Laaser, J. E. Charge Density and Hydrophobicity-Dominated Regimes in the Phase Behavior of Complex Coacervates. *ACS Macro Lett.* **2021**, *10* (8), 1029−1034.

(19) Liu, Y.; Santa Chalarca, C. F.; Carmean, R. N.; Olson, R. A.; Madinya, J.; Sumerlin, B. S.; Sing, C. E.; Emrick, T.; Perry, S. L. Effect of Polymer Chemistry on the Linear Viscoelasticity of Complex Coacervates. *Macromolecules* **2020**, *53* (18), 7851−7864.

(20) Larson, R. G.; Liu, Y.; Li, H. Linear viscoelasticity and time-temperature-salt and other superpositions in polyelectrolyte coacervates. *J. Rheol.* **2021**, *65* (1), 77−102.
(21) Fu, J.; Schlenoff, J. B. Driving forces for oppositely charged polyion association in aqueous solutions: enthalpic, entropic, but not electrostatic. *J. Am. Chem. Soc.* **2016**, *138* (3), 980−990.
(22) Chang, L.-W.; Lytle, T. K.; Radhakrishna, M.; Madinya, J. J.; Vélez, J.; Sing, C. E.; Perry, S. L. Sequence and entropy-based control of complex coacervates. *Nat. Commun.* **2017**, *8* (1), 1273.
(23) Lytle, T. K.; Chang, L.-W.; Markiewicz, N.; Perry, S. L.; Sing, C. E. Designing electrostatic interactions via polyelectrolyte monomer sequence. *ACS central science* **2019**, *5* (4), 709−718.
(24) Chremos, A.; Douglas, J. F. Counter-ion distribution around flexible polyelectrolytes having different molecular architecture. *Soft Matter* **2016**, *12* (11), 2932−2941.
(25) Rahalkar, A.; Wei, G.; Nieuwendaal, R.; Prabhu, V. M.; Srivastava, S.; Levi, A. E.; De Pablo, J. J.; Tirrell, M. V. Effect of temperature on the structure and dynamics of triblock polyelectrolyte gels. *J. Chem. Phys.* **2018**, *149* (16), na DOI: 10.1063/1.5035083.
(26) Krogstad, D. V.; Lynd, N. A.; Choi, S. H.; Spruell, J. M.; Hawker, C. J.; Kramer, E. J.; Tirrell, M. V. Effects of polymer and salt concentration on the structure and properties of triblock copolymer coacervate hydrogels. *Macromolecules* **2013**, *46* (4), 1512−1518.
(27) Srivastava, S.; Andreev, M.; Levi, A. E.; Goldfeld, D. J.; Mao, J.; Heller, W. T.; Prabhu, V. M.; De Pablo, J. J.; Tirrell, M. V. Gel phase formation in dilute triblock copolyelectrolyte complexes. *Nat. Commun.* **2017**, *8*, na DOI: 10.1038/ncomms14131.
(28) Lou, J.; Friedowitz, S.; Qin, J.; Xia, Y. Tunable coacervation of well-defined homologous polyanions and polycations by local polarity. *ACS central science* **2019**, *5* (3), 549−557.
(29) Muzammil, E. M.; Khan, A.; Stuparu, M. C. Post-polymerization modification reactions of poly (glycidyl methacrylate) s. *RSC Adv.* **2017**, *7* (88), 55874−55884.
(30) Hatton, F. L.; Derry, M. J.; Armes, S. P. Rational synthesis of epoxy-functional spheres, worms and vesicles by RAFT aqueous emulsion polymerisation of glycidyl methacrylate. *Polym. Chem.* **2020**, *11* (39), 6343−6355.
(31) Stuparu, M. C.; Khan, A. Thiol-epoxy "click" chemistry: Application in preparation and postpolymerization modification of polymers. *J. Polym. Sci., Part A: Polym. Chem.* **2016**, *54* (19), 3057−3070.
(32) Gadwal, I.; Stuparu, M. C.; Khan, A. Homopolymer bifunctionalization through sequential thiol−epoxy and esterification reactions: an optimization, quantification, and structural elucidation study. *Polym. Chem.* **2015**, *6* (8), 1393−1404.
(33) Kubo, T.; Easterling, C. P.; Olson, R. A.; Sumerlin, B. S. Synthesis of multifunctional homopolymers via sequential post-polymerization reactions. *Polym. Chem.* **2018**, *9* (37), 4605−4610.
(34) Buerkli, C.; Lee, S. H.; Moroz, E.; Stuparu, M. C.; Leroux, J.-C.; Khan, A. Amphipathic homopolymers for siRNA delivery: probing impact of bifunctional polymer composition on transfection. *Biomacromolecules* **2014**, *15* (5), 1707−1715.
(35) Zhu, Z.; Jeong, G.; Kim, S. J.; Gadwal, I.; Choe, Y.; Bang, J.; Oh, M. K.; Khan, A.; Rao, J. Balancing antimicrobial performance with hemocompatibility in amphiphilic homopolymers. *J. Polym. Sci., Part A: Polym. Chem.* **2018**, *56* (21), 2391−2396.
(36) Wang, Q.; Schlenoff, J. B. The polyelectrolyte complex/coacervate continuum. *Macromolecules* **2014**, *47* (9), 3108−3116.
(37) Li, L.; Srivastava, S.; Andreev, M.; Marciel, A. B.; de Pablo, J. J.; Tirrell, M. V. Phase Behavior and Salt Partitioning in Polyelectrolyte Complex Coacervates. *Macromolecules* **2018**, *51* (8), 2988−2995.
(38) Meng, S.; Ting, J. M.; Wu, H.; Tirrell, M. V. Solid-to-Liquid Phase Transition in Polyelectrolyte Complexes. *Macromolecules* **2020**, *53* (18), 7944−7953.
(39) Vieregg, J. R.; Lueckheide, M.; Marciel, A. B.; Leon, L.; Bologna, A. J.; Rivera, J. R.; Tirrell, M. V. Oligonucleotide-Peptide Complexes: Phase Control by Hybridization. *J. Am. Chem. Soc.* **2018**, *140* (5), 1632−1638.
(40) Spruijt, E.; Cohen Stuart, M. A.; van der Gucht, J. Linear viscoelasticity of polyelectrolyte complex coacervates. *Macromolecules* **2013**, *46* (4), 1633−1641.
(41) Rubinstein, M.; Colby, R. H. *Polymer Physics*; Oxford University Press: New York, 2003.
(42) Tang, S.; Wang, M.; Olsen, B. D. Anomalous self-diffusion and sticky Rouse dynamics in associative protein hydrogels. *J. Am. Chem. Soc.* **2015**, *137* (11), 3946−3957.
(43) Fetters, L. J.; Kiss, A. D.; Pearson, D. S.; Quack, G. F.; Vitus, F. J. Rheological behavior of star-shaped polymers. *Macromolecules* **1993**, *26* (4), 647−654.

https://doi.org/10.1021/acsmacrolett.4c00167
ACS Macro Lett. 2024, 13, 688−694